Transactions of the 17th International Conference on Structural Mechanics in Reactor Technology (SMiRT 17)
Prague, Czech Republic, August 17 –22, 2003
Paper # K03-1

Effect of Irregular Topography on Strong Ground Motion Amplification

Tetsushi KURITA[1)], Tadashi ANNAKA[1)], Satoru TAKAHASHI[2)], Masayoshi SHIMADA[1)] and Toshio SUEHIRO[2)]

1) Tokyo Electric Power Services Co., Ltd., Tokyo, Japan
2) Tokyo Electric Power Company, Tokyo, Japan

ABSTRACT

Topographic irregularities such as hills affect the amplification characteristics of strong ground motion. Due to the interference between direct waves and scattered waves, the behavior of seismic waves passing through irregular terrain is complex. In this study, records of seismic ground motion were compared to simulated seismic waves, calculated from 3-dimensional FEM. The study objectives were to build an analytical model capable of accurately reproducing the observed data and to evaluate the amplification characteristics of strong ground motion in areas characterized by irregular topography.

KEY WORDS: Irregular Topography, Strong Ground Motion, Amplification Characteristics, 3-dimensional FEM, Array Observation System, Numerical Simulation, Earthquake Observation Records.

INTRODUCTION

In contrast to most other civil structures, electric power facilities are often found in hilly terrain, since power generation facilities tend to be built at locations remote from the areas in which the power is consumed. The characteristics of seismic waves at such sites are significant factors in the design, maintenance, and seismic-performance of these facilities.

The amplification characteristics of topographic irregularities such as hills are known to be intricate, due to the coupling of X, Y, and Z components. However, few studies, either analytical or experimental, have closely examined this particular issue. In the handful of earlier studies performed to date [1],[2],[3], researchers were unable to closely examine the characteristics of amplification beneath the ground surface, due to their lack of access to dense array observation systems.

Since 1982, Tokyo Electric Power Company has gathered and recorded seismic records using an array system installed at a hill in Yokosuka, Japan. The compiled data is stored in a database. In this study, a numerical simulation was carried out using 3-dimensional FEM based on seismic records for the eastward offshore earthquake in Chiba Prefecture (M_J=6.7), which occurred December 17, 1987. The data collected on this earthquake represents the largest cluster of data for a single event in the database. This study sought to evaluate the effects of irregular topography on the amplification characteristics of strong ground motion, based on numerical simulations.

ARRAY OBSERVATION SYSTEM

Fig. 1 shows a cross-section of the target hill and the installed seismographs. The elevation of the hilltop is about 80 meters. The vertical array system consists of seismographs buried at three depths below the surface of the hill top. Other seismographs are installed in the hillside and at the bottom of the hill. The No. 5 seismograph at the bottom of the hill is positioned on horizontal rock. Each tri-axial seismograph consists of two horizontal components and one vertical component. The No. 1 seismograph is the trigger for the array observation system. The five seismographs are arranged along a line in the same horizontal plane.

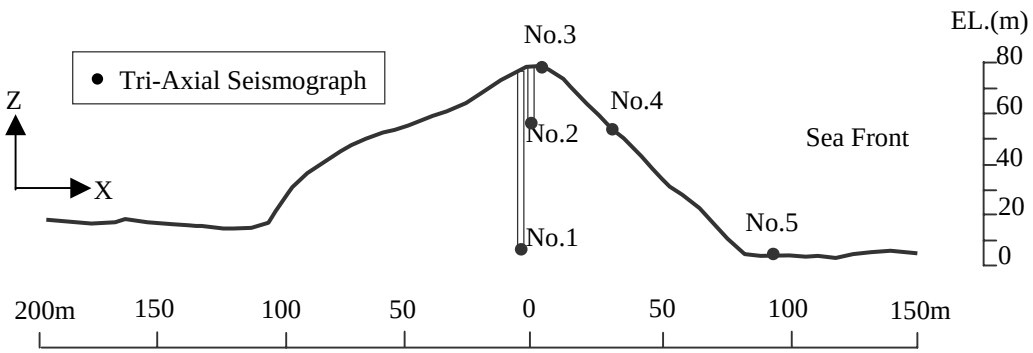

Fig. 1 Cross-section of target hill and installed seismographs

The soil properties at the objective site were obtained from the drilling survey described in Table 1. Although the target hill is basically rocky, a very thin weathered layer is present on the surface. Since the observation point represented by the No.5 seismograph is considered to be close to free field, it was used as a control point to invert incident waves for numerical simulation.

Table 1. Soil properties obtained from drilling survey

Layer No.	Depth (m)	Thickness (m)	Geology	P-Wave Velocity (m/s)	S-Wave Velocity (m/s)	Density (g/cm^3)
1	-4	4	Silty Mudstone	1600	250	1.7
2	-8	4	Silty Mudstone	1600	400	1.8
3	-18	10	Mudstone	1900	600	1.9
4	-58	30	Sandstone	2000	700	1.9
5	-66	8	Sandy Tuff	2000	700	1.9
6	infinite	-	Tuff	2000	700	1.9

Table 2. Objective earhquake data and observed maximum acceleration at hilltop

Event No.	Origin Time	Focal Depth (km)	M_J	Location of Epicenter	Max. Acc. at Hilltop (cm/s^2)		
					X	Y	Z
EQ.066	87/12/17 11:08:16.8	58	6.7	Offshore of Chiba Prefecture	132.4	122.4	53.9
EQ.070	88/08/12 14:14:53.9	69	5.3	Southern Boso Peninsula	85.7	65.1	33.0
EQ.083	89/10/14 06:19:58.6	21	5.7	Inshore of Izu-oshima Island	35.1	89.4	7.7
EQ.154	94/06/29 11:01:58.8	60	5.2	Southern Boso Peninsula	88.0	106.3	29.3
EQ.164	95/07/03 08:53:23.2	122	5.2	Sagami Bay	61.9	43.4	22.9

M_J means the Japan Meteorological Agency magnitude.

Table 2 lists various earthquakes for analysis and their peak accelerations at the hilltop. These represent the major events recorded in the database. The most significant event data recorded represents the earthquake occurring eastward offshore of Chiba Prefecture. In the table, this event is indicated as EQ.66.

ANALYSIS OF OBSERVATION DATA

Fig. 2 shows distributions of peak acceleration against elevation. For horizontal components, peak acceleration increases dramatically at the hilltop. This tendency is not seen for the vertical component. The peak accelerations at the surface are fairly similar to those observed underground.

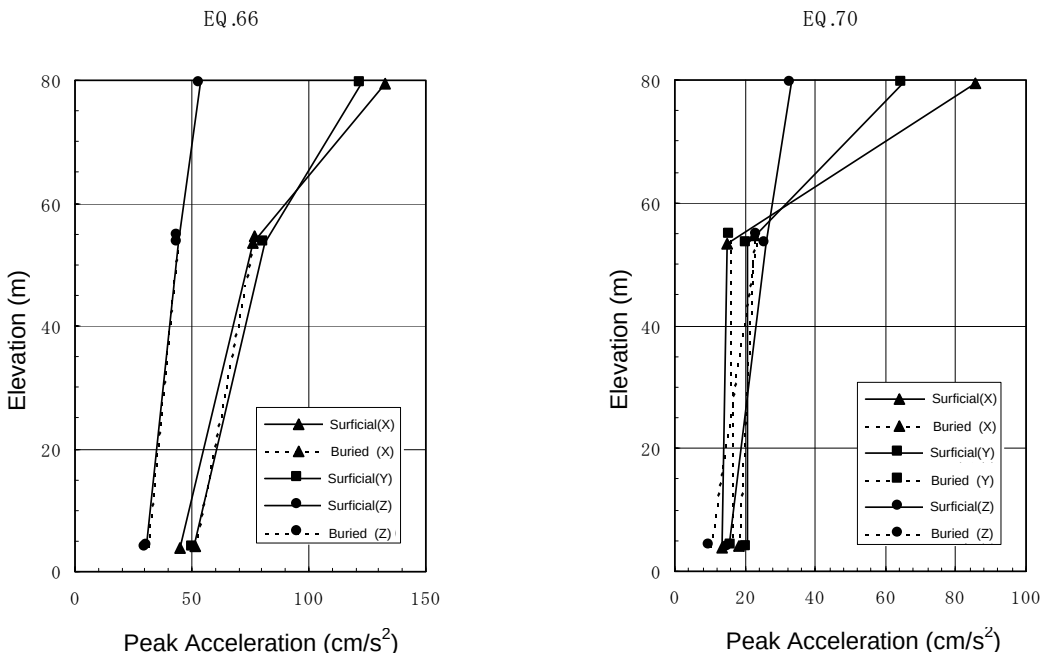

(1) EQ.66 (2) EQ.70

Fig. 2 Distribution of peak acceleration against elevation

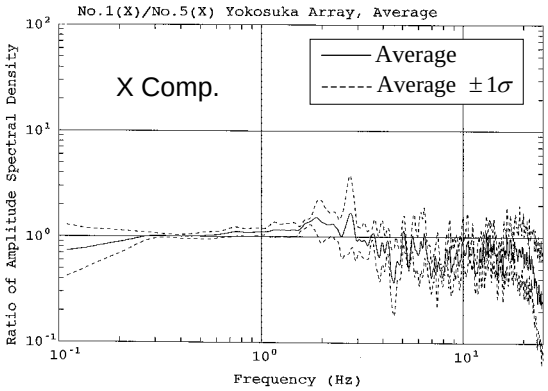

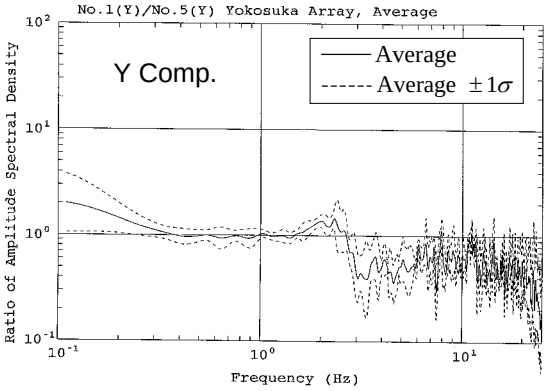

(1) No.1/No.5

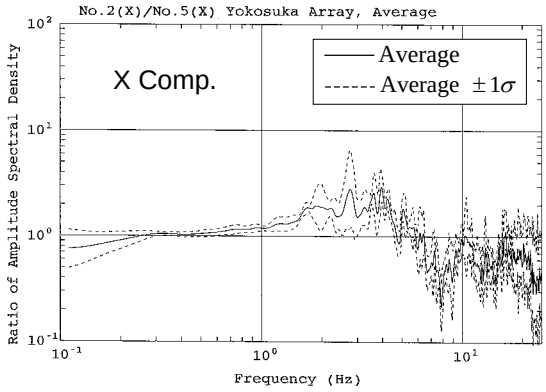

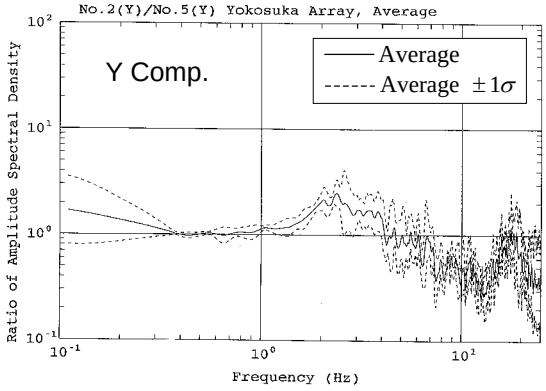

(2) No.2/No.5

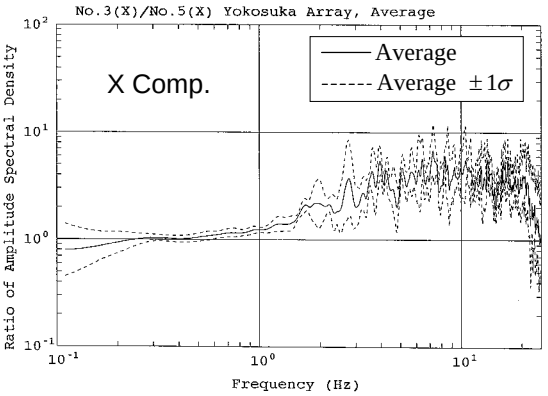

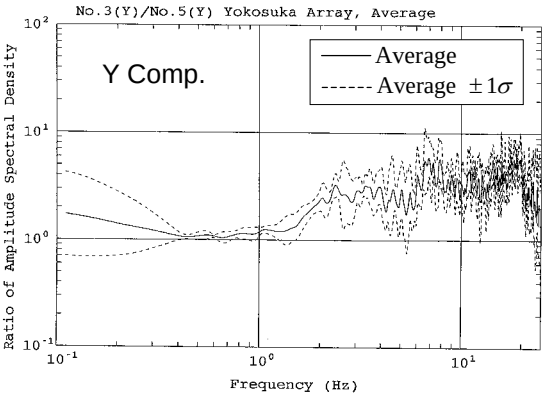

(3) No.3/No.5

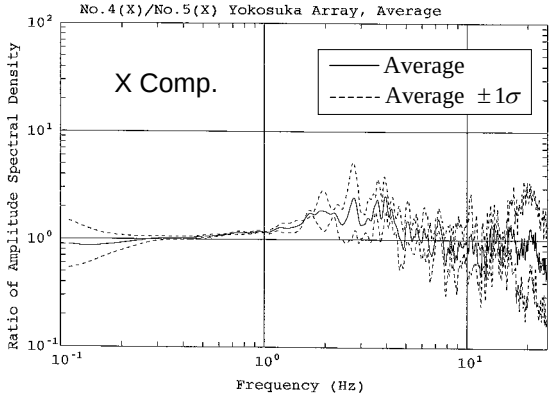

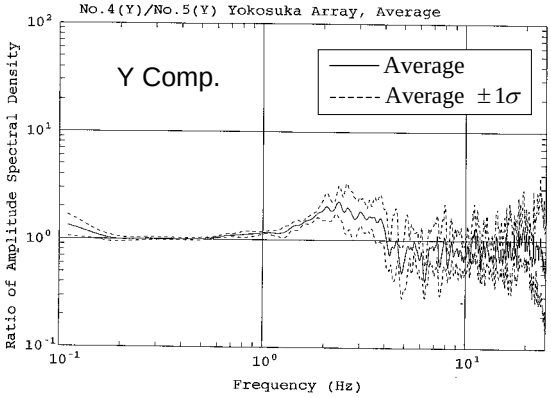

(4) No.4/No.5

Fig. 3 Averaged Fourier spectral ratio

Fig. 3 shows the geometric averaged Fourier spectral ratio at each observation point with respect to the reference point located in the free field (No. 5). After smoothing of each acceleration Fourier spectrum with a Parzen window of 0.2 Hz, the ratios were calculated. This was followed by geometric averaging. The entire hill has a rocky substrate, with a thin weathered layer on the surface. The effect on acceleration of the discontinuity between the substrate and the weathered layer is negligible, because the latter is very thin. In this figure, solid lines indicate averages, while dotted lines indicate "average ± standard deviation." The amplitude ratio at the hilltop is largest, some four to five times that of the free field wave. This large gain is attributed to the focusing of waves at the hilltop. In the spectral ratio of the No. 1 seismograph, the amplification ratio of the low frequency side below 3 Hz equals 1.0, while that of the high frequency side is less than 1.0. The component of the direct wave in this frequency band is believed to be cancelled by the reflected waves occurring within the hill, since the No. 1 seismograph is located just under the crest. On the other hand, the upper part above 2Hz in the Fourier spectral ratio of No. 3 seismograph is amplified. This phenomenon continues to about 20 Hz. The amplification ratio increases, because the reflected waves focus at the hilltop.

NUMERICAL SIMULATION

Analytical Conditions

Numerical simulation was carried out using 3-dimensional FEM with the analytical model shown in Fig. 4. The boundary conditions at the bottom and sides were viscous, with 2-dimensional dashpots. In the side boundaries, dashpots were placed between 2-dimensional free-field models and a 3-dimensional FE model. The 3-dimensional model was composed of eight-node solid elements. Incident waves acted along the two horizontal components and the vertical component.

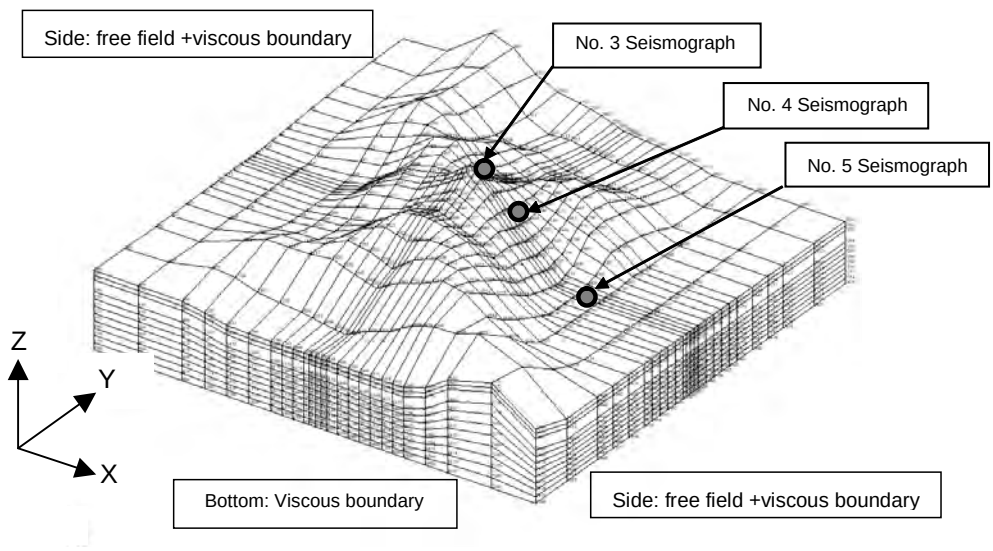

Fig. 4 Three-dimensional FE model

Deconvoluted waves based on the following equation in the frequency domain with acceleration records observed at the No. 5 seismograph were used as incident waves. The incident plane was regarded to be EL. -50m.

$$\mathbf{I}(\omega) = \mathbf{H}^{-1}(\omega) \cdot \mathbf{R}(\omega) \tag{1}$$

here,

$\mathbf{I}(\omega) = \{I_X, \quad I_Y, \quad I_Z\}^T$: incident wave

$\mathbf{R}(\omega) = \{R_{5X}, \quad R_{5Y}, \quad R_{5Z}\}^T$: observed record at No.5

$\mathbf{H}(\omega) = \begin{bmatrix} H_{5X/X} & H_{5X/Y} & H_{5X/Z} \\ H_{5Y/X} & H_{5Y/Y} & H_{5Z/Y} \\ H_{5Z/X} & H_{5Z/Y} & H_{5Z/Z} \end{bmatrix}$: theoritical transfer function of response at No.5 seismograph against incident wave, in which previous analytical model is employed

This equation can be used to obtain neutral incident waves, which do not contain the effects of topographic irregularity.

The soil properties in Table 1 were applied to construct the FE model. The damping matrix was given by Rayleigh damping, with $h = 1\%$ at the control points $f_0 = 2.24Hz$ and $f_1 = 13.0Hz$.

Verification of Numerical Simulation

Fig. 5 shows a comparison of Fourier spectral ratios in the X component between the simulated results and observed records. These spectral ratios are amplification ratios for the incident wave in the X direction. In this figure, both analytical values and observed values were smoothed with a bandwidth of 0.2 Hz. Both spectra are in good agreement, confirming that the analytical model is capable of modeling the behavior of the actual hill topography. In particular, the simulation replicates the amplification observed at the crest, in which amplification ratios above 5 Hz are about ten and over. The simulation also expresses the reduced amplification cancelled by the scattering waves at special underground points No. 1 and 2, just under the hilltop.

Fig. 6 compares the simulated Fourier spectra against observed data. Both spectra were smoothed by a Parzen window with bandwidth of 0.2 Hz. Fig. 7 shows a comparison of acceleration time histories in the X component between simulated and observed data. In this figure, solid lines indicate analytical results, while dotted lines indicate the observed data. The simulated results agree well with the observed data, confirming the accuracy of the simulation.

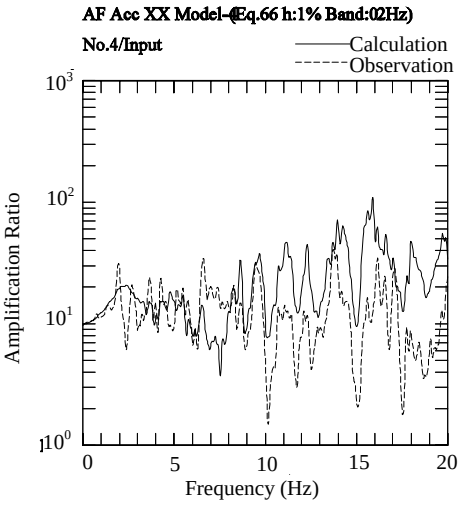

(4) Response at No.4 /Incident wave

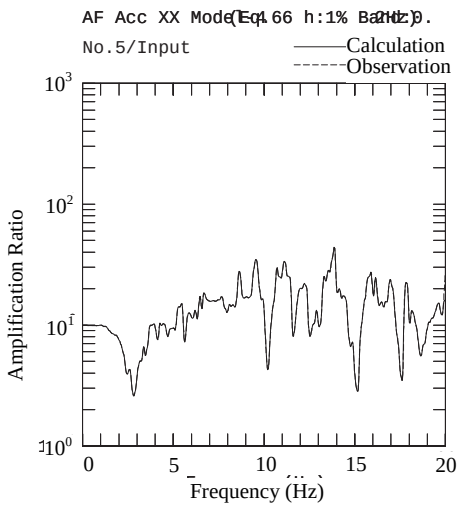

(5) Response at No.5 /Incident wave

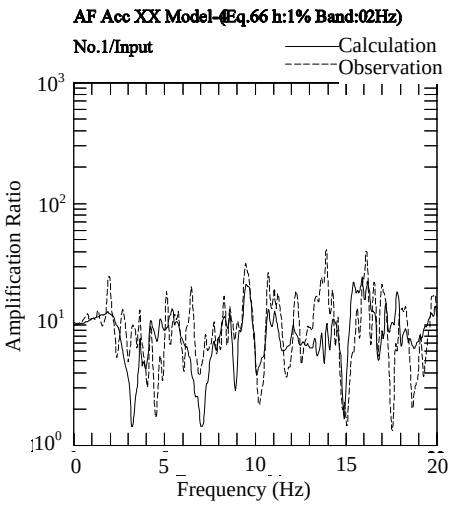

(1) Response at No.1 /Incident wave

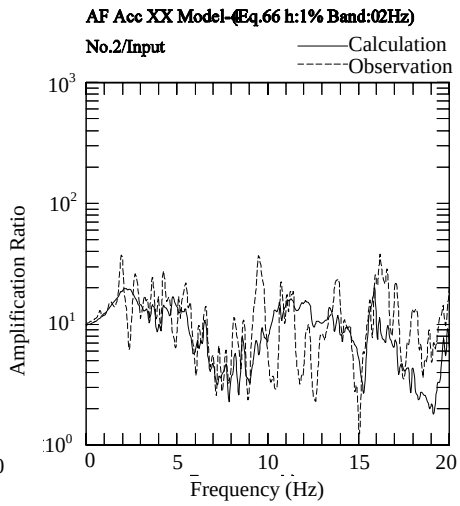

(2) Response at No.2 /Incident wave

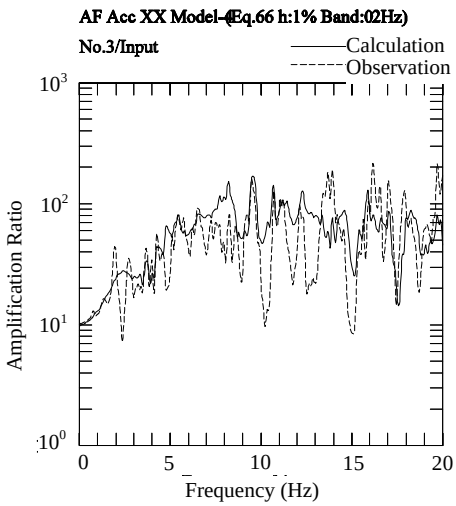

(3) Response at No.3 /Incident wave

Fig.5 Comparison of Fourier spectral ratio between observed data and simulated response

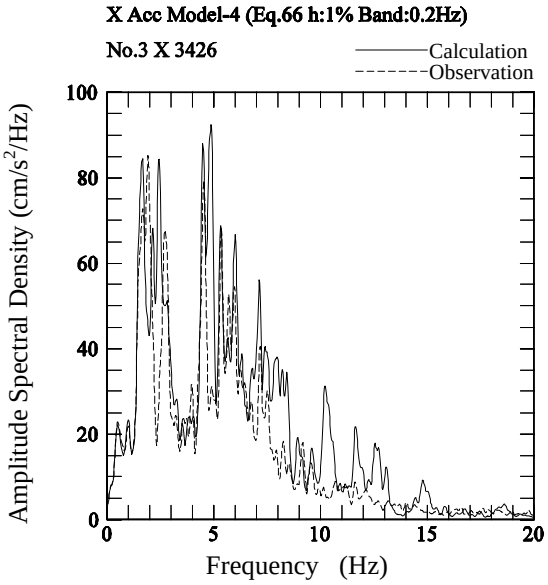

(3) No.3

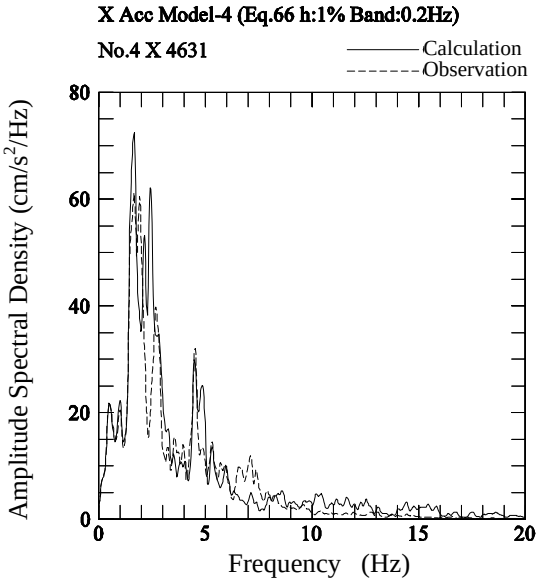

(4) No.4

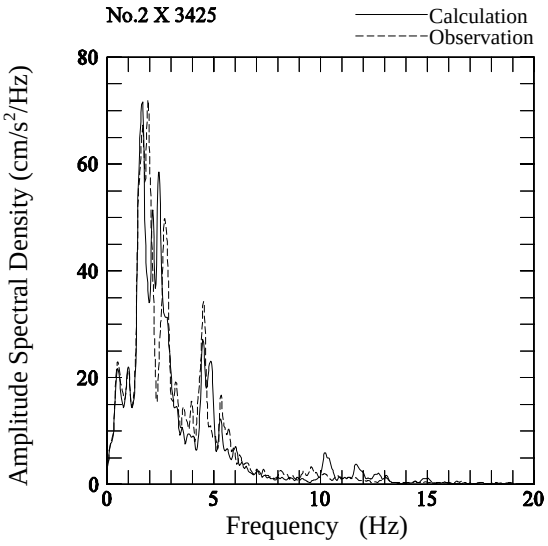

(2) No.2

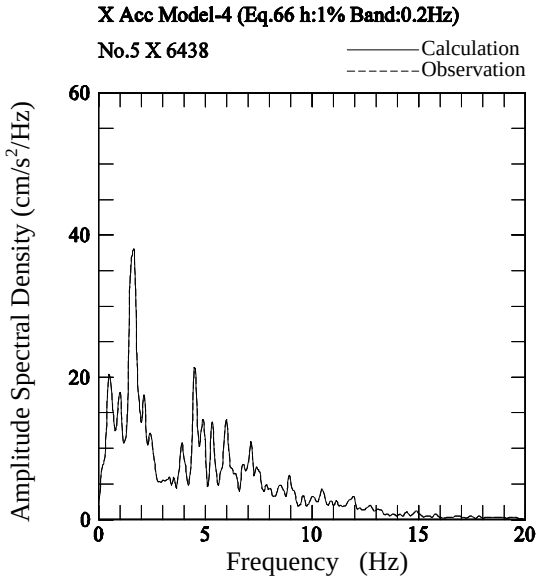

(5) No.5

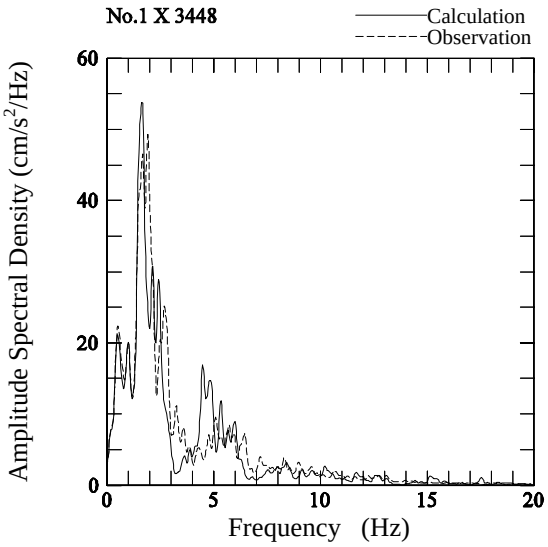

(1) No.1

Fig.6 Comparison of Fourier spectra between observed data and simulated response (X-comp.). Both spectra are smoothed by a Parzen window with bandwidth of 0.2 Hz.

Feature of Strong Ground Motion due to Irregular Topography

The beginning of this section discussed an investigation of the phenomenon of seismic wave cancellation by wave scattering. Fig. 8 shows the distribution of band-pass filtered acceleration vectors at a targeted frequency, as indicated in Fig. 5(1) by amplification reduced to 1.0 or less. The targeted frequency of the filter is 3.27Hz. As shown in this figure, the amplitude near the location of the No. 1 seismograph is significantly less than at other points. This appears to be the node of vibration.

The amplification characteristics due to the shape of the hill were then investigated. Fig. 9 displays the distribution of the maximum acceleration vectors in the X-Z plane (Y=0.0m). The incident wave, occurring along the X direction only, was a Ricker wavelet with center frequency of 10Hz and maximum amplitude of 10 cm/s^2. This figure shows a plot of the maximum vectors obtained at each node of the FE model. The figure indicates a very large increase in the amplification at the crest. Moreover, the amplitudes along the plane of the steep slope, which is seaward and includes the No.4 seismograph, are relatively small. On the other hand, very large amplification is seen in the gentle slope on the opposite side. These results support the contention that amplification characteristics depend on the shape of a slope.

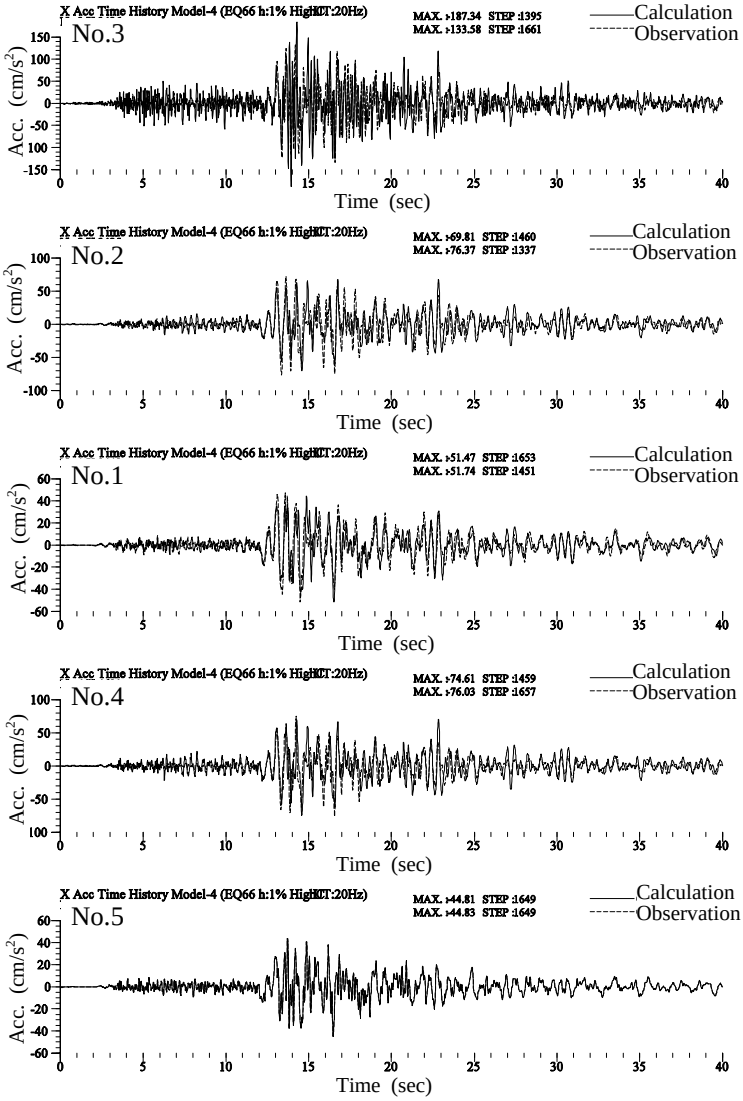

Fig. 7 Comparison of time history between observed data and simulated response (X-comp.)

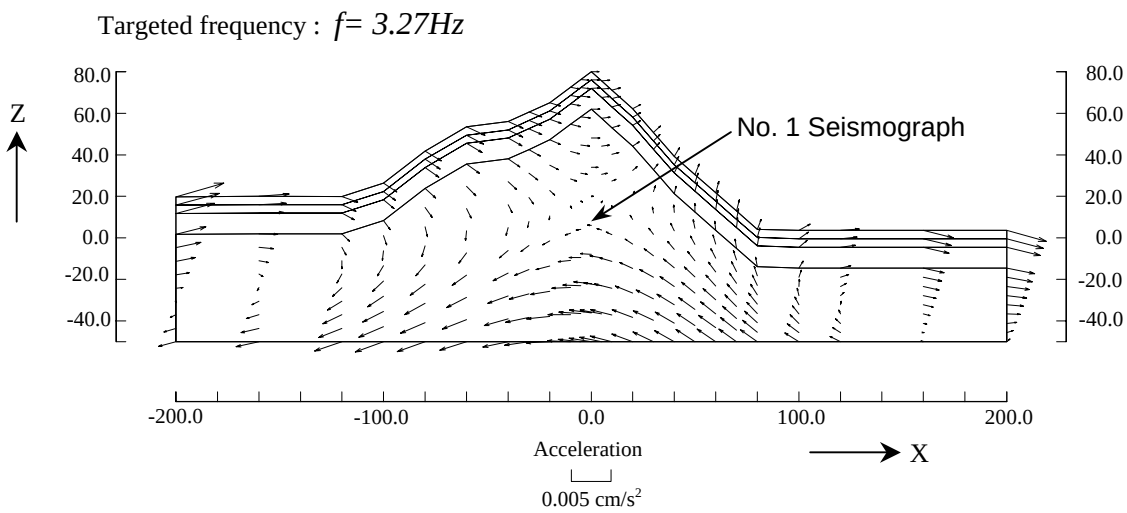

Fig. 8 Distribution of acceleration vector, focusing on a specific frequency: *f*=3.27Hz (X-Z cross section, Y=0.0m)

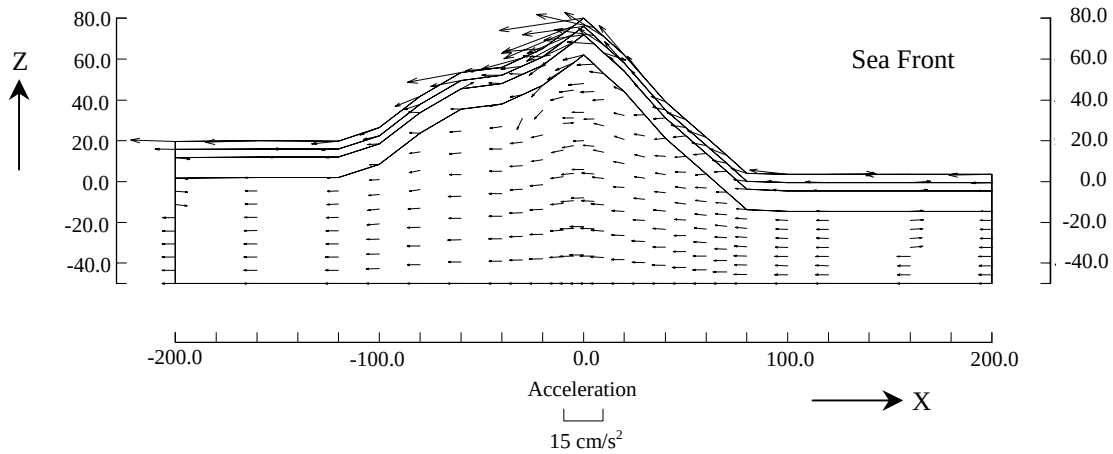

Fig. 9 Distribution of maximum acceleration vector (X-Z cross section, Y=0.0m)

CONCLUSIONS

A numerical simulation of array observation records was performed using 3-dimensional FEM to grasp the effects of irregular topography on the amplification characteristics of strong motion. The conclusions obtained in this study are given below:

1) The preparation of a detailed, carefully prepared numerical model enables accurate simulation of observed data.
2) Three-dimensional FEM successfully simulated the characteristics of large amplification at hilltop caused by focused reflected waves.
3) For a special frequency in the transfer function, in which the amplification was reduced to 1.0 or less, the location at the seismograph just under the crest is the node of the vibration.
4) The amplification varies, depending on the shape of the hill slope.

REFERENCES

1. Kanda, K. and Motosaka, M., “The evaluation of effects of spatial variability of soil properties, surface topography and spatial coherency of incident wave on ground motion amplification –The case of Kushiro J.M.A. site-” (in Japanese), *Journal of Structural and Construction Engineering, AIJ*, No. 476, 1995, pp.85-94.
2. Ishida, H., Sasaki, T., Niwa, M., Kitagawa, Y. and Kashima, T., “Amplification characteristics of surface layers obtained from earthquake observation records of vertical instrument arrays at Kushiro local meteorological observatory” (in Japanese), *Journal of Structural and Construction Engineering, AIJ*, No. 490, 1996, pp.91-100.
3. Paolucci, R., “Amplification of earthquake ground motion by steep topographic irregularities”, *Earthquake Engineering and Structural Dynamics*, No. 31, 2002, pp.1831-1853.